

NASA Project Apollo Working Paper No. 1064

PROJECT APOLLO

EXTERNAL PRESSURE BUCKLING OF THIN

CONICAL FRUSTUMS OF 30° HALF ANGLE

FACILITY FORM 602

N70-76238	
(ACCESSION NUMBER)	(THRU)
72	NONE
(PAGES)	(CODE)
TMX-65230	
(NASA CR OR TMX OR AD NUMBER)	(CATEGORY)

[REDACTED]

NATIONAL AERONAUTICS AND SPACE ADMINISTRATION

MANNED SPACECRAFT CENTER

HOUSTON, TEXAS

December 12, 1962


NASA PROJECT APOLLO WORKING PAPER NO. 1064

PROJECT APOLLO

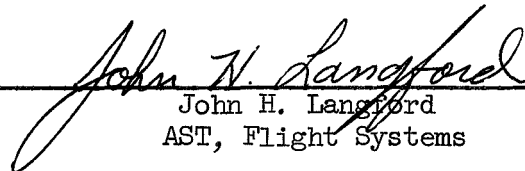
EXTERNAL PRESSURE BUCKLING OF THIN

CONICAL FRUSTUMS OF 30° HALF ANGLE


Prepared by:



David Brown
AST, Flight Systems



John H. Langford
AST, Flight Systems



Robert H. McDonnell
AST, Flight Systems

Authorized for Distribution:



Maxime A. Faget
Assistant Director, Research and Development

NATIONAL AERONAUTICS AND SPACE ADMINISTRATION

MANNED SPACECRAFT CENTER

HOUSTON, TEXAS

December 12, 1962

ACKNOWLEDGEMENTS

Use of part of the Lockheed Stress Memorandum (Ref. 1) in this paper is hereby acknowledged. The authors are grateful to Mr. E. Wilson for valuable help received in building the test specimens and in conducting the tests.

TABLE OF CONTENTS

Section		Page
1.0	SUMMARY	1 - 1
2.0	INTRODUCTION	2 - 1
3.0	SYMBOLS	3 - 1
4.0	DISCUSSION OF PUBLISHED ANALYTICAL DATA	4 - 1
	4.1 Ultimate external pressure	4 - 1
	4.2 Initial external buckling pressure	4 - 2
5.0	EXPERIMENTAL INVESTIGATIONS	5 - 1
	5.1 Test setup	5 - 1
	5.2 Discussion of test results	5 - 1
	5.3 Standardization of test results	5 - 2
6.0	COMPARISON OF AVAILABLE ANALYTICAL METHODS WITH TEST RESULTS	6 - 1
	6.1 Ultimate pressure	6 - 1
	6.2 Initial external buckling pressure	6 - 1
7.0	RECOMMENDATIONS AND CONCLUSIONS	7 - 1
	7.1 Prediction of initial external buckling pressure	7 - 1
	7.2 Prediction of ultimate pressure	7 - 1
	7.3 Prediction of permanent set	7 - 1
	7.4 Selection of design pressures	7 - 2
	7.5 General recommendations	7 - 2
8.0	REFERENCES	8 - 1

LIST OF TABLES

Table		Page
1	SUMMARY OF CONFIGURATIONS TESTED AND MATERIAL PROPERTIES	9 - 1
2	TEST RESULTS SPECIMEN NO. 2.	9 - 2
3	TEST RESULTS SPECIMEN NO. 3.	9 - 4
4	TEST RESULTS SPECIMEN NO. 4.	9 - 6
5	TEST RESULTS SPECIMEN NO. 5.	9 - 9
6	TEST RESULTS SPECIMEN NO. 6.	9 - 11
7	TEST RESULTS SPECIMEN NO. 7.	9 - 13
8	TEST RESULTS SPECIMEN NO. 8.	9 - 16
9	TEST RESULTS SPECIMEN NO. 9.	9 - 18
10	TEST RESULTS SPECIMEN NO. 10	9 - 20
11	TEST RESULTS SPECIMEN NO. 11	9 - 21
12	TEST RESULTS SPECIMEN NO. 12	9 - 23
13	TENSILE TEST RESULTS	9 - 25
14	STANDARDIZATION OF TEST RESULTS	9 - 27
15	COMPARISON OF ULTIMATE PRESSURES	9 - 28
16	COMPARISON OF INITIAL BUCKLING PRESSURES	9 - 29
17	PERCENTAGE VARIATION BETWEEN TEST AND THEORETICAL RESULTS.	9 - 30

LIST OF FIGURES

Figure		Page
1	Plot of thickness-radius-length parameter vs K_L . .	10 - 1
2	Plot of non-dimensional shape factor vs critical-compressive stress ratio	10 - 2
3	Comparison of available analytical data on 30° half angle conical frustums	10 - 3
4	External buckling pressure coefficient vs length-radius-thickness parameter	10 - 4
5	Typical test setup	10 - 5
6	Test arrangement	10 - 6
7	Elastic buckles in cylindrical specimen	10 - 7
8	Buckle pattern on stiffened shell	10 - 7
9	Failure of lower bay together with permanent set in upper bay	10 - 8
10	Interaction of buckle patterns on multi-bay specimen	10 - 8
11	Permanent buckle after release of pressure	10 - 9
12	Failure of stainless steel specimen	10 - 9
13	Initial buckling pressures vs no. of circumferential buckles based on Seide's exact formula for multi-bay conical shell (specimen no. 8) showing test results	10 - 10
14	Comparison of ultimate pressure between experimental and theoretical results	10 - 11
15	Comparison of initial buckling pressure between experimental and theoretical results. (Lower edge of test range taken as initial buckling pressure).	10 - 12
16	Design curve for determining initial buckling pressure on 30° half angle conical frustums using "Hart's" method	10 - 13

EXTERNAL PRESSURE BUCKLING OF THIN
CONICAL FRUSTUMS OF 30° HALF-ANGLE

1.0 SUMMARY

Tests were conducted on several conical frustums of 30° half-angle under external pressure to determine the initial external buckling pressure and the ultimate external pressure and to determine what portions of the existing published data are applicable to the type of pressure cabin considered for Apollo-type spacecraft. A suggested design curve is presented for the determination of the initial external buckling pressure on non-stiffened conical frustums of 30° half-angle.

2.0 INTRODUCTION

One design considered for the pressure cabin of Apollo-type spacecraft consists of a thin, ring stiffened aluminum shell, part of which is a conical frustum of 30° half-angle. For certain design conditions, it is necessary that the shell be capable of withstanding external pressure, and it is therefore desirable that methods be available for predicting both the initial buckling pressure and the post buckling strength of this type of structure. Several solutions are available for predicting the initial external buckling pressure on conical frustums, but there is a wide variation of results and opinion amongst the authors. Only one method was found for predicting the ultimate external pressure on conical frustums, and this is given in reference 1.

The purpose of this paper is to determine which, if any, of the available methods can best be used to determine both the initial external buckling pressure and the ultimate external pressure on conical frustums of 30° half-angle. To do this, a limited amount of testing was conducted using three different materials, 2024-T3 clad aluminum alloy, fully hardened AISI 301 stainless steel, and annealed AISI 302 stainless steel. The parameters were varied to investigate the effects of changing sheet thickness and cone height, and of inserting an intermediate frame.

3.0 SYMBOLS

E	Young's modulus of shell wall material
F_{cy}	Yield strength of material in compression
F_{tu}	Ultimate strength of material in tension
F_{ty}	Yield strength of material in tension
I	Moment of inertia
L	Axial length of cylinder or cone
L'	Slant length of cone
n	Number of circumferential waves in cone buckled by external pressure
\bar{n}	Number of circumferential waves in equivalent cylinder buckled under external pressure
P	Uniform external pressure
P_b	Initial buckling pressure
P_e	Initial buckling pressure for equivalent cylinder
P_s	Permanent set pressure
P_u	Ultimate pressure
R	Radius of cylinder
R_1	Radius of small end of conical frustum
R_2	Radius of large end of conical frustum
R_{av}	Average radius of conical frustum
t	Shell wall thickness
α	Semi-vertex angle of cone
ν	Poisson's ratio of shell wall materials

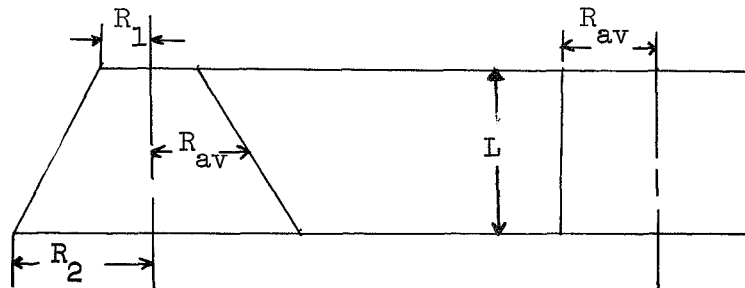
Page 3 - 2

ρ_1	Radius of curvature of conical frustums at $\frac{1}{2} L$
ρ	Radius of curvature of conical frustum at large end
K	Non-dimensional shape factor

4.0 DISCUSSION OF PUBLISHED ANALYTICAL DATA

The various methods for predicting the initial external buckling pressure and the ultimate external pressure are examined to determine their exactness in the range of conical frustums of 30° half-angle considered for the pressure cabin of Apollo-type spacecraft.

- 4.1 Ultimate external pressure. - The only method found for predicting the ultimate external pressure on conical frustums of 30° half-angle was the "Lockheed" method, ref. 1. This solution was developed for cylinders under external pressure but may be used by utilizing an appropriate equivalent cylinder. Initial investigation showed that the best accuracy was obtained with the equivalent cylinder shown below.



The "Lockheed" method given in ref. 1, for predicting the ultimate external pressure, is as follows:

$$P_u = \frac{K_1 F_{cr} t}{R_{av}}$$

$$\text{where } F_{cr} = K_2 E (t/L)^2$$

where K_1 is obtained from figure 1 and K_2 is obtained from figure 2 of this report.

Note: Figures 1 and 2 were replotted from ref. 1. This reference does not show test data, but suggests that because of imperfections in construction, the ultimate external pressure predicted by this method be reduced by 10 percent.

4.2 Initial external buckling pressure. - Several solutions are available for predicting the initial external buckling pressure on conical frustums and are discussed below. Figure 3 is a plot of each of these methods with previous test data, where available. Also, the range of parameters applicable to Apollo-type spacecraft pressure cabins are noted.

4.2.1 "Seide's" methods, refs. 2 and 3. - Seide has published two methods for predicting the initial external buckling pressure on conical frustums.

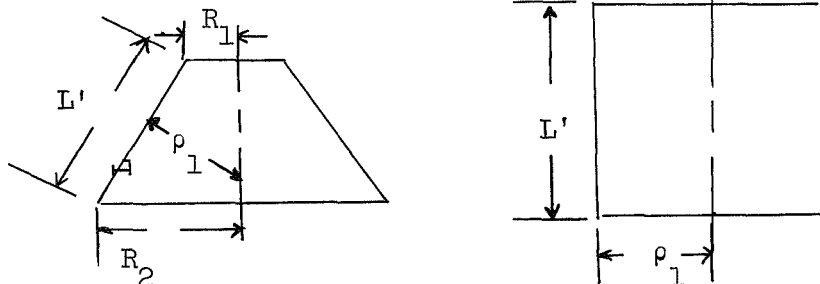
"Seide's Approximate" formula,

$$P_b = \frac{.92E}{\left(L'/\rho_1\right)\left(\rho_1/t\right)^{5/2}} \quad \text{Ref. 2.,}$$

and "Seide's Exact" solution,

$$P_b = \frac{\pi^2 E \left(t/\rho_1\right)^3 \left(\rho_1/L'\right)^2}{12(1-\nu^2) \left[1/2 + (nL'/\pi\rho_1)^2\right]} \left\{ \left[1 + (nL'/\pi\rho_1)^2\right]^2 + \frac{12(1-\nu^2)(L'/t\rho_1)^2}{\pi^4 \left[1 + (nL'/\pi\rho_1)^2\right]^2} \right\} \quad \text{Ref. 3.,}$$

are based on the equivalent cylinder shown below.



"Seide's Exact" formula is difficult to use in that the number of circumferential buckles must be known to determine the minimum initial external buckling pressure. Both of Seide's methods are plotted in figure 3 along with test data from references 2 and 3. As can be seen, good agreement was obtained between the two methods.

- 4.2.2 "NACA TR-874" method, ref. 4. - This solution is an approximate one developed at the U. S. Experimental Model Basin for cylinders under external pressure, but may be used on cones if the cones are replaced by the same equivalent cylinder as in the Seide method. This formula,

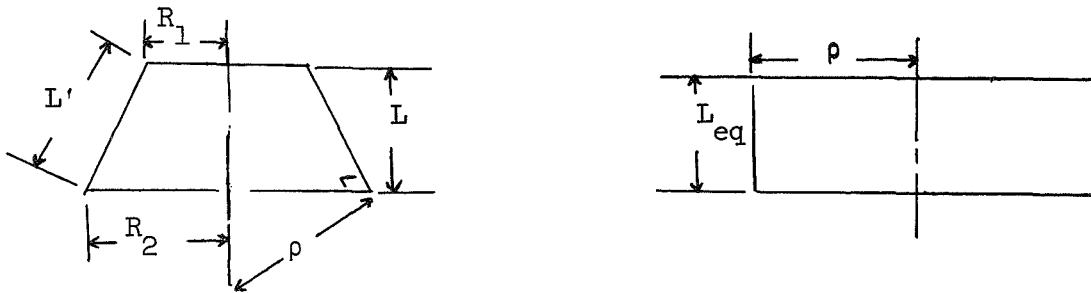
$$P_b = \frac{2.42E (t/2 \rho_1)^{5/2}}{(1 - \nu^2)^{3/4} \left[L'/2 \rho_1 - .45 (t/2 \rho_1) \right]^{1/2}},$$

has a marked resemblance to "Seide's Approximate" formula except for the Poisson's ratio term and the $.45(t/2 \rho_1)^{1/2}$ term. On examination, it was determined that $.45(t/2 \rho_1)^{1/2}$ was small relative to $L'/2 \rho_1$ and therefore could be neglected. By substituting $\nu = .3$ into the above equation and neglecting $.45(t/2 \rho_1)^{1/2}$ the above equation reduces to "Seide's Approximate" equation,

$$P_b = \frac{.92E}{(L'/\rho_1) (\rho_1/t)^{5/2}},$$

Because of the similarity between these formulas the NACA TR-874 formula was not plotted.

- 4.2.3 "Hart" method, ref. 5. - This method for determining the initial external buckling pressure uses another equivalent cylinder as follows:



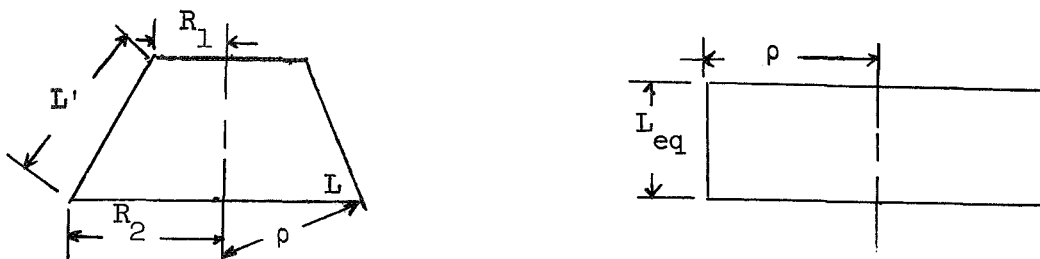
$$\text{where } L_{eq} = \frac{.75 R_1 + 1.45 R_2}{2.2 R_2} (L')$$

The expression for initial buckling as given in this reference is:

$$P_b = \frac{C_p E \pi^2}{12(1 - \nu^2) (L_{eq}/\rho)^2 (\nu/t)^3}$$

where C_p is a buckling coefficient shown plotted in figure 4. This figure was replotted from reference 5 and includes a 90 percent probability factor which Hart states was determined from previous tests. This 90 percent probability factor means that 90 percent of all test results fall above that predicted by Hart's equation. The results, as shown in figure 3, are lower than the results by the other methods.

4.2.4 "Bijlaard" method, ref. 6. - Using this method, the initial external buckling pressure may be calculated by replacing the conical shell with an equivalent cylinder as shown below:



$$\text{where } L_{eq} = \frac{R_1 + 1.2 R_2}{2.2 R_2} (L')$$

The equation for predicting the initial external buckling pressure,

$$P_b = \frac{.92 E(t/\rho)^{5/2}}{L_{eq}/\rho - 0.657(t/\rho)^{1/2}}$$

is only valid if,

$$H = 8.91 / \left(L_{eq} / \sqrt{t\rho} \right)^4 < .111,$$

which is the case for the range of specimens tested. Figure 3 shows a plot of this method along with the others for comparison.

5.0 EXPERIMENTAL INVESTIGATIONS

- 5.1 Test setup. - The test setup is shown in figures 5 and 6. The pressure differential was produced by evacuating the interior of the test specimen with a "Duo-Seal" vacuum pump driven by a $\frac{1}{2}$ H.P. electric motor. The differential pressure was registered on a dial gauge reading inches of mercury. The rate of pressure variation was controlled very accurately by means of the two valves shown in figure 6. It was possible to stop the pump very quickly at the moment of collapse of the specimen by tripping the motor switch, so that excessive damage to the specimen was not caused.

Each conical shell was formed in one piece by rolling the developed shape. The single lap joint was closed by one row of rivets. One-half inch was allowed for this lap joint, and a projected $\frac{3}{4}$ inch width was left at top and bottom to allow for clamping. The riveted joint was sealed by inner and outer beads of non-hardening plastic materials, as were all other joints on the assembled test specimen.

The clamping rings were fabricated from $\frac{3}{4}$ inch plywood. The top closing plate was $\frac{1}{4}$ inch thick aluminum alloy while the whole specimen was mounted on a $\frac{3}{8}$ inch steel plate. The geometries of the test specimens were designed to simulate a portion of the Apollo Command Module cabin, and, because of the method of applying load, a reasonably low failing pressure had to be built into the specimens while using standard sheet-metal gauges. Table 1 shows the specimen configurations and the material properties for each specimen tested. All specimens were unstiffened with the exception of specimen no. 4 which had four heavy, equally spaced longitudinal stiffeners riveted to the outside of the shell.

- 5.2 Discussion of test results. -

- 5.2.1 Initial buckling. - Some of the cones which were made from thicker sheet or from steel became completely buckled very suddenly. But with most of the specimens it was difficult to establish the criterion of initial buckling, since there was a considerable range between the pressure (P_i) to cause the first buckle, and the pressure (P_s) at which a complete and

stable buckle pattern had developed. For the purposes of this paper, "initial buckling" was taken as being P_{i1} . The test results on all specimens are shown in tables 2 through 12.

- 5.2.2 Permanent set. - In the absence of instrumentation to determine the onset of permanent set, reliance was placed entirely on the observers' sense of feel and sight. It was possible to feel slight ridges with the fingertips before these became large enough to be obvious to the naked eye. Because permanent set occurs largely at the nodal points between buckles, and the buckle pattern is not always the same at each successive pressurization, it is difficult to instrument for this phenomenon.
- 5.2.3 Ultimate pressure. - With the exception of specimen no. 4 which was stiffened and specimen no. 12, the methods of pumping and sealing proved adequate to achieve failure. With most of the cones the onset of failure was quite gradual, so that the ultimate pressure could be read accurately. Just prior to failure, the ridges between the buckles had formed well-defined "columns" and in all cases failure appeared to be caused by local instability of these columns. Figures 7 through 12 show photographs of several specimens at various phases during the tests.
- 5.2.4 Interaction of buckle patterns between two adjacent bays. - Two specimens were tested which had a reinforcing ring located at $L/2$. The test results on one of these specimens (no. 8) are shown in figure 13. The points marked P_{bu} and P_{bL} are the initial buckling pressure on the upper and lower bays respectively of specimen no. 8. The point marked P_{bc} is the pressure at which the lower and upper buckle pattern merged to form a stable buckle pattern for the multi-bay conical shell (specimen no. 8). Also shown is a plot of initial external buckling pressure for the upper and lower bays taken as separate conical frustums using Seide's exact formula, ref. 3. As can be noted, P_{bc} , the pressure at which a combined stable buckle pattern forms and P_{bu} , the upper bay buckling pressure are both higher than P_{bL} , the lower bay buckling pressure.
- 5.3 Standardization of test results. - All of the test results were factored to bring them in line with standard geometries and material properties, in order to compare them with the theoretical results. For this purpose, transverse and longitudinal tensile specimens were made from the sheet material of the

various conical specimens and tested to determine the actual material properties. The results of the pull tests are shown in table 13.

"Seide's Approximate" formula,

$$P_b = \frac{.92 E}{(L'/\rho_1)(\rho_1/t)^{5/2}}, \quad (\text{Ref. 2})$$

was used to factor the initial buckling values, since it was shown that this formula presents quite well the values obtained in the tests. These standardized values are shown in table 14.

6.0 COMPARISON OF AVAILABLE ANALYTICAL METHODS WITH TEST RESULTS

- 6.1 Ultimate pressure. - The "Lockheed" method was the only solution found for predicting the ultimate external pressure on conical frustums of 30° half-angle. The results, as presented in table 15 and figure 14, are in good agreement with the test results for most of the specimens.
- 6.2 Initial external buckling pressure. - The various methods for predicting the initial external buckling pressure and test results are shown in table 16 and figure 15. "Hart's" method gives the best correlation for predicting the initial external buckling pressure on non-stiffened 30° half-angle conical frustums, for most of the specimens. However, there is some scatter around Hart's results due to manufacturing imperfections. Table 17 gives the percentage variation between test and theory for the methods considered.

7.0 RECOMMENDATIONS AND CONCLUSIONS

- 7.1 Prediction of initial external buckling pressure.- On the basis of the results obtained during the test, "Hart's" formula,

$$P_b = \frac{C_p E \pi^2}{12(1-\nu^2)(L_{eq}/\rho/t)^3},$$

is the best method for determining the initial external buckling pressure on non-stiffened 30° half-angle conical frustums. As discussed previously, this method has a 90 percent probability factor included, which means that 90 percent of all test data fall above the predicted results. The percentage variation as shown in table 17 indicate that an additional 10 percent reduction is necessary to account for test scatter due to imperfections in construction. The altered Hart equation,

$$P_b = \frac{.90 C_p \pi^2 E}{12(1-\nu^2)(L_{eq}/\rho)^2(\rho/t)^3}$$

is plotted on figure 16 to be used as a design curve for predicting the initial external buckling pressure on non-stiffened 30° half-angle conical frustums.

- 7.2 Prediction of ultimate pressure.- For the prediction of ultimate pressure, "Lockheed's" method is the only one available. This formula gives good agreement with test and is suggested for use in determining the ultimate external buckling pressure on non-stiffened 30° half-angle conical frustums. However, there is approximately a 6 percent scatter band on the lower side of the theoretical results for 9 out of 10 specimens. Therefore, it is suggested that a factor of .94 be used on the Lockheed formula, that is:

$$P_u = \frac{.94 K_2 F_{cr} t}{R_{av}}.$$

- 7.3 Prediction of permanent set.- No method was found which calculated this criterion and, as has been mentioned earlier, it is even difficult to recognize the point at which permanent set is obtained on test. It is highly desirable that this situation should be rectified by further testing, which should be done on a much broader scale than was available for this work.

- 7.4 Selection of design pressures. - In all of the tests, the ultimate pressure was at least twice the initial buckling pressure. So that, purely on a strength basis, the current practice of designing pressure vessels using the initial buckling pressure as the ultimate pressure is very conservative. There are some cases, such as escape during a booster explosion, where the ultimate criterion by itself may be quite satisfactory, even though the pressure vessel may have been loaded beyond the point of permanent set, and would have to be scrapped. But there are obviously other cases, such as traveling through the region of maximum dynamic pressure, where permanent damage to the pressure vessel could not be tolerated, and the criterion of permanent set would be the most logical one to use for design purposes. Once again, it is emphasized that more testing is necessary before this criterion can be fully determined.
- 7.5 General recommendations. - Although, with the reservations mentioned above, some of these methods are adequate for initial design purposes, a specimen of the full scale structure should always be subjected to ultimate test. It has been shown (see paragraph 5.2(a)) that it is safe to check the bay of largest diameter on a multi-bay constant thickness shell, although more work needs to be done in this direction, using more parameters as variables.

8.0 REFERENCES

1. "Cylindrical Ducts and Tanks Under External Crushing Pressure," August 1, 1947. Lockheed Aircraft Corp. Stress Memo No. 96.
2. Morgan, E. J., Seide, P., and Weingarten, V. I.: "Semiannual Report on the Development of Design Criteria for Elastic Stability of Thin Shell Structures." Space Technology Laboratories, Inc., Report No. STL/TR-59-0000-09959, July 1, 1959, to December 31, 1959.
3. Morgan, E. J., Seide, P., and Weingarten, V. I.: "Final Report on Development of Design Criteria for Elastic Stability of Thin Shell Structures, December 31, 1960." STL Report No. TR-60-0000-19425.
4. Batdorf, S. B.: "A Simplified Method of Elastic-Stability Analysis for Thin Cylindrical Shells." NACA TR-874, 1947.
5. Hart, T. J.: "Design Criteria and Analysis for Thin-Walled Pressurized Vessels and Interstage Structures." ARS Preprint No. 1099-60.
6. Bijlaard, P. P.: "Critical External Pressure of Conical Shells that are Simply Supported at the Edges." February 1953. Bell Aircraft Corporation Report No. 02-941-027.

9.0 TABLES

TABLE 1.- SUMMARY OF CONFIGURATIONS TESTED AND MATERIAL PROPERTIES

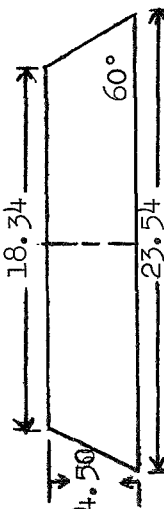
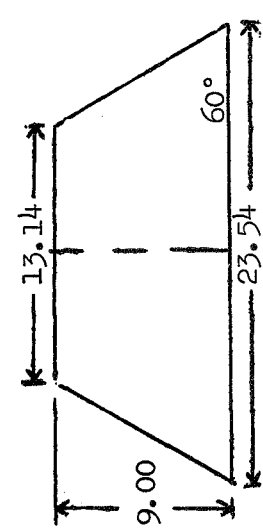
Cone No	2	3	4	5	6	9	10	12	
Configuration									
Material	2024-T3 CIAD AL				2024-T3 CIAD AL				301 F. H. Stainless
Thickness	.020				.020				025
E x 10-6	10				10				26
Ftu x 10-3	.25				.25				185
									.16
	</								

TABLE 2.- TEST RESULTS SPECIMEN NO. 2.

Psi	No. of Buckles	Width of Buckle	Depth of Buckle	Remarks
1.72 .98 0	3			Initial buckles-around joint Buckles out
1.23 1.72 1.92 1.96 0	4 7 8	3.5		Buckle beside joint 2 buckles each side of joint
1.13 1.96 2.21	1 7 10	5		
2.33 0	13	$4\frac{1}{2}$ - 5		Buckles all the way around cone No set
2.06	13	$4\frac{1}{2}$ - 5		Buckles all around
2.33 2.70	13 13	$4\frac{1}{2}$ - 5		Buckles very uniform except 2 at joint and one opposite joint (small one)
1.47 0				Buckles popped out No set
1.47 1.96 3.19	1 13			All buckles in Buckles very uniform except 2 at joint and one opposite joint (small one)

TABLE 2.- Cont'd.

Psi	No. of Buckles	Width of Buckle	Depth of Buckle	Remarks	
0	13	6	$\frac{1}{8}$	First noticeable permanent set	
1.72				All buckles in	
3.68				Buckles deeper	
.64				Buckles popped out	
0		6	$\frac{1}{8}$	More pronounced set. 1" flat either side of some ridges	
1.84				All buckles in	
3.93					
4.18					
1.47		6.5	$\frac{1}{8}$	1st buckle popped out	
.59				Last buckle popped out	
0				Definite permanent set - 1" flat on each side of ridges	
1.72				All buckles in	
4.42	13	6.5	$\frac{1}{4}$		
4.91					
1.47		3.5		1st buckle popped out	
0				One buckle next to joint stayed in. Ridge lines very pronounced.	
5.03				Ridges between buckles very distinct. Skin pulling in slightly more to either side of columns.	
5.16	13	3.5			
5.26	12			Cone collapsed.	

TABLE 3.- TEST RESULTS SPECIMEN NO. 3.

Psi	No. of Buckles	Width of Buckle (In)	Depth of Buckle (In)	Remarks
1.67 0	2	3	.03	No set
1.47	2			
1.62	3			
1.92	8			
1.96	9			
2.19	13		.03	
.98 0	0			No set
.98	1			
1.84	13			
2.70	13			
1.60	12			1st buckle out
0				Slight set near joint - 1" flat
.74	1			
1.72	13			
2.95	13	5 - 6	.03	
0				$1\frac{1}{2}$ " of flat, and slightly concave near joint
.61	1			
1.72	13			
3.19	13			
0				
3.49	13		.05	

TABLE 3.- Cont't.

Psi	No. of Buckles	Width of Buckle (In)	Depth of Buckle (In)	Remarks
0	13			$2\frac{1}{2}$ " concave buckle near joint
1.47				
3.68				2nd point of permanent set ($\frac{3}{8}$ " flat). Full buckle left
3.93	13		.07	
0				3 or 4 ridges discernible
4.18	13	$3\frac{1}{2}$ - $6\frac{1}{2}$		$1\frac{3}{4}$ " rad. on ridges
0				Definite permanent set all round
4.42				Radius of ridges - $1\frac{1}{4}$ " to $1\frac{1}{2}$ "
0	12			At 1 psi all buckles out except two at joint. All ridges very well defined.
.88				3rd buckle popped in
4.67				$1\frac{1}{8}$ " rad on ridge
0				
4.91	12		$\frac{1}{8}$	Nearly failed. $1\frac{1}{8}$ " rad on ridge
0				
5.13				Failed

TABLE 4.- TEST RESULTS SPECIMEN NO. 4.

Psi	No. of Buckles	Width of Buckle (In)	Depth of Buckle (In)	Remarks
0				
.98	1			Beside joint stiffener
1.72	2			Same bay as above
0	0			
.74	1			
1.67	2			
2.01	4			
2.16	9			3 buckles in each of 3 bays, none in other bay
0	0			1st buckle to appear is still in very faintly
.79	1			Buckle #1 just in
.59	0			Buckle #1 just out
0				
.74	1			
1.52	2			
1.92	8			Number of buckles in each bay - 4, 3, 1, 0
2.06	13			4, 3, 3, 3
2.41	12			3, 3, 3, 3
1.87				1st buckle out
0	(1)			All buckles out except one (slightly)
1.47	10			4, 3, 3, 0
2.21	12			3, 3, 3, 3
2.70	12			

TABLE 4.- Cont'd.

Psi	No. of Buckles	Width of Buckle (In)	Depth of Buckle (In)	Remarks
0	(1)	5	.02	1st permanent set (2nd buckle)
2.95	12			
1.72	Few			
0				No definite permanent set - very slight only
3.19	12	5	.03	
0				No definite permanent set - very slight only
.49	2			
1.57	2			
1.96	10, 13			4, 3, 3, 0 then 4, 3, 3, 3
2.11	12			3, 3, 3, 3
3.44	12			rad. 3" - 4"
1.47	1			
0				
3.68	12			rad. still > 2"
0				Permanent set in 3 or 4 places
4.18	12	$3\frac{1}{2}$, $5\frac{1}{2}$ & $5\frac{1}{2}$	0.46	2" - $2\frac{1}{2}$ ", undeflected at stiffener 2" rad.
4.67	12			
0				Still not very much set
4.91	12			
5.16	12			2" rad.

TABLE 4.- Cont'd.

Psi	No. of Buckles	Width of Buckle (In)	Depth of Buckle (In)	Remarks
5.40	12			
0				Definite set at all buckles
5.89	12			2" rad
6.48				
6.39				$\frac{1}{4}$ deflection on top plate
6.88				
7.02				
7.37				Ridge S-bending ($\frac{3}{8}$ " deflection of top plate)
7.86				
8.35				
8.84				
9.33				
9.82				
10.02				Sprang a leak
0				Photo
10.46				Sprang a leak
0				Not failed - test discontinued.

TABLE 5.- TEST RESULTS SPECIMEN NO. 5.

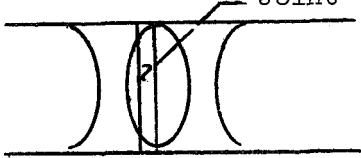
Psi	No. of Buckles	Width of Buckle (In)	Depth of Buckle (In)	Remarks
0				Slight initial flat near joint*
1.11	8			
.76	0			
0				No set except*
1.03	8	7	$\frac{3}{64}$	Joint 
1.23	8	7	$\frac{3}{64}$	
.69-.64	0			
0				No set
.98	8	7	$\frac{1}{16}$	
1.35				
.69-.61				
0				No set
.91	1			
.98	8			
1.47	8	$7\frac{1}{2}$	$\frac{5}{64}$	2" rad on ridges
.66-.54				
0	0			No set
.93	1			
.98	8			
1.60	8	$7\frac{1}{2}$	$\frac{5}{64}$	$1\frac{3}{4}$ " rad. on ridges

TABLE 5.- Cont'd.


Psi	No. of Buckles	Width of Buckle (In)	Depth of Buckle (In)	Remarks
0	0			No set
.96	8			
1.72	8			$1\frac{1}{2}$ " rad. on ridges
0	0			Permanent set just discernible
.93	8			
1.84	8	$8\frac{1}{4}$	$\frac{1}{16}$ -0	$1\frac{1}{2}$ " rad. Section thru buckle: 
0	0			Permanent set just noticeable at all of eight ridges
.93	8			
1.96	8	$8\frac{1}{4}$ - $8\frac{3}{4}$ "	$\frac{3}{32}$ - $\frac{1}{32}$	1" rad on ridges
.32	1			
0	0			Most definitely permanent set
2.21	8	$8\frac{1}{2}$.2 max. $\frac{1}{16}$ at max. buckle width	$\frac{3}{4}$ " rad. on ridges at max. buckle width
2.46	8			
0	1			1 buckle in permanently
3.00				Ridges begin to fall over
3.14				Failed

TABLE 6.- TEST RESULTS SPECIMEN NO. 6.

Psi	No. of Buckles	Width of Buckle (In)	Depth of Buckle (In)	Remarks
.86	1			Initial buckle at joint
1.18	3			
1.23	9			2 small buckles by joint
1.28	9	$7\frac{1}{2}$ " max.		
.84				First buckle out
.56				All buckles out
0				Set faintly discernible
1.08	9	$7\frac{1}{2}$ " max.	.04	
1.47	9	$5\frac{1}{2}$ " - 8		Width of seven buckles - 7" to 8", small buckles $5\frac{1}{2}$ " & $6\frac{1}{2}$ "
1.72	9		$\frac{3}{32}$	
.74				First buckle out
.27				All buckles out
0				Slight permanent set
.88 - .98	9			Buckles in
1.96	7	$7\frac{1}{2}$ " - 10	$\frac{1}{8}$	Ridge rad. - 1", 2-10 buckles
.54				First buckle out
0	1			Definite permanent set, permanent buckle

TABLE 6.- Cont'd.

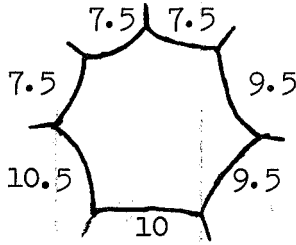
Psi	No. of Buckles	Width of Buckle (In)	Depth of Buckle (In)	Remarks
1.96 0 2.70 3.09	7			 <p>BUCKLE WIDTH</p> <p>Ridges going over, ridge rad. = 1" Failed</p>

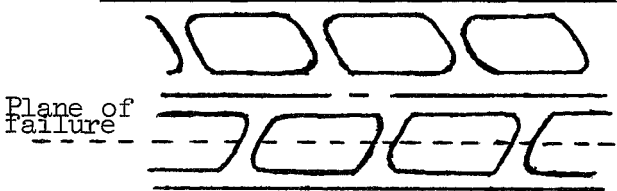
TABLE 7.- TEST RESULTS SPECIMEN NO. 7

Psi	No. of Buckles		Width of Buckle (In)	Depth of Buckle (In)	Remarks
	U	L			
0					
1.42		1			
1.47		2			
1.72		5			Last buckle formed beside joint
1.96		5			
.74		0			
0					
1.23		1			
1.47		4			
1.72		6			
1.96		6			
2.11		9			Upper bay joint going in
2.25		12			
2.45	4	14			Top joint in middle of buckle
1.86	1	14			
.74	0	0			
0					
1.23		1			
2.11	2	?			
2.21	4	?			
2.5	7	14			
2.75	8	13			
1.27					Last top buckle out

TABLE 7.- Cont'd.

Psi	No. of Buckles		Width of Buckle (In)	Depth of Buckle (In)	Remarks
	U*	L			
.74	0	0			Last bottom buckle out No set
1.23	0	1			
1.96	1	?			Note: $\frac{1}{4}$ of lower buckle lines up with ridge of upper buckle and vice versa
2.94	10	10			
3.06					
1.03					Last top buckle out
.74					Last bottom buckle out Permanent set noticeable at bottom, none on top
2.94	10	10	7 L $4\frac{1}{4}$ - $5\frac{1}{4}$ U	.04 L .04 U	Ridge rad. $1\frac{1}{4}$ " top and bottom
3.24	10	10			Permanent set just noticeable at top, more distinct at bottom
3.43	10	10		$\frac{1}{16}$ L & U	Ridge rad. - 1" to $1\frac{1}{4}$ " Slightly more set U & L than after 6.6
3.68	10	10			Permanent set easily visible on bottom, but not on top
1.96	10	10			

TABLE 7.- Cont'd.

Psi	No. of Buckles		Width of Buckle (In)	Depth of Buckle (In)	Remarks
	U	L			
3.43	10	10	$7\frac{1}{4}$ L		
3.92	10	10	$7\frac{1}{4}$ L $5\frac{1}{2}$ U	$\frac{1}{16}$ L & U	Lower buckles going rectangular 1" ridge rad. U & L
4.46					Set easily visible U & L
.59	0	0			$\frac{3}{4}$ " ridge rad.
5.7					Whole ridge-line pattern visible just prior to failure
					Failure
					

NOTE: U & L means upper and lower bays respectively.

TABLE 8.- TEST RESULTS SPECIMEN NO. 8.

Psi	No. of Buckles		Width of Buckle	Depth of Buckle	Remarks
	U*	L			
0					
1.91		1			Higher than P for first buckle on # 7 because this cone is more uniform
2.06		3			
2.16		7			
2.30		12			
2.35	3	14			
0					No set
1.91		1			
1.96		7			
2.16	1	14			
2.45	4	14			
2.75	7	14			
2.94	8	14			
0					No set
2.94	8	14			
3.28	10	12			
0					Slight set lower bay, none upper
2.89	10	12			
3.53	10	12			
0					More set lower bay, slight in upper
3.58	11	11			
3.92	11	11			
0					Set definitely visible, U and L

TABLE 8.- Cont'd.

Psi	No. of Buckles		Width of Buckle	Depth of Buckle	Remarks
	U*	L			
2.84	11	11			
4.41	11	11			
0					More set
4.90	11	11			
0					Yet more set
5.64					Failure

NOTE: U & L means upper and lower bays respectively.

TABLE 9.- TEST RESULTS SPECIMEN NO. 9.

Psi	No. of Buckles	Width of Buckle	Depth of Buckle	Remarks
0				
4.22	8	$6\frac{1}{2}$ - 8	.04	All buckles in at once - very suddenly
2.30	0			
0				
3.63	8			As above
2.28	0			
3.58	8			As above
4.46	8	$6\frac{1}{2}$ - 8	.07	
2.18	0			
3.53	8			As above
4.90	8	$6\frac{1}{2}$ - 8	.1	2" - $2\frac{1}{2}$ " ridge rad.
2.08	0			Two buckles slow going out
0				
3.48	8			
5.39	8	7 - 8	.125	2" ridge rad.
2.03	0			Two buckles slow going out
0				Set faintly discernible
3.48	8			
5.98	8	7 - $8\frac{1}{2}$		
0	0			Set can be felt at all ridges, but not seen
3.38	8			

TABLE 9.- Cont'd.


Psi	No. of Buckles	Width of Buckle	Depth of Buckle	Remarks
6.42	8	$7\frac{1}{2}$ -	.155	Buckles going trapezoidal
1.50	0	$8\frac{1}{2}$		Very definite set - easily seen $\frac{1}{2}$ " flat to either side of ridges
0				
7.40	8			Buckles leaning over:- 
0	1	9		Buckle permanently in - all ridge lines plainly visible
1.67	3			
2.21	8			
8.97	8			Failure

TABLE 10.- TEST RESULTS SPECIMEN NO. 10

Psi	No. of Buckles	Width of Buckle	Depth of Buckle	Results
0				
2.84				
0				(Returned to zero for first photo)
3.09	1			Buckle right on joint
3.14	8	$7\frac{1}{2}$.03	
.39	6			
.20	5			
0	5			Permanent set easily visible after buckles were pushed out manually
1.96	8			
3.92	8			1" ridge rad.
4.90	8			Very hard, straight ridges
5.10	8			Ridges tilting over
5.29	8			Failure

TABLE 11.- TEST RESULTS SPECIMEN NO. 11.

Psi	No. of Buckles	Width of Buckle	Depth of Buckle	Remarks
0				Joint has slight flat
4.27	1			Joint
0				No set
3.98	1			Joint
4.52	9	7		Buckles all around
2.90	3			
2.85	0			
0				No set
3.59	1			Joint
4.08	9	7		
4.96	9	7	$\frac{1}{16}$	
0				No set
3.59	1			Joint
3.93	9			
5.40	9	7	$\frac{1}{16}$	
0				
3.54	1			
3.83	9			
5.89	9	7	$\frac{1}{16}$	
0				Slight set
6.39	9	7	$\frac{3}{32}$	2" ridge rad.
0				Definite permanent set

TABLE 11.- Cont'd.

Psi	No. of Buckles	Width of Buckle	Depth of Buckle	Remarks
6.88	9	6 - $7\frac{1}{2}$	$\frac{1}{8}$	2" ridge rad.
0				Ridge lines pronounced
7.37	9			
0				
11.30	9			
11.89				Failure

TABLE 12.- TEST RESULTS SPECIMEN NO. 12.

Psi	No. of Buckles	Width of Buckle	Depth of Buckle	Remarks
0				Slight flat at joint
6.14	8			All buckles in at once
3.88	0			
0				No set
5.99	8			
6.63	8	7	$\frac{1}{16}$	
0				
5.85	8			
7.12	8			
0				No set
7.62	8	7	$\frac{1}{16}$	
0				No set
5.80	8			
8.11	8			
0				No set
8.60	8	7	$\frac{1}{16}$	Ridge rad. = 2"
0				No set
9.09	8			
0				No set
9.58				No set
0				
10.07	8			Looks as if 2 buckles will become 1 buckle

TABLE 12.- Cont'd.

Psi	No. of Buckles	Width of Buckle	Depth of Buckle	Remarks
10.12	7	11	$\frac{1}{8}$	Definite permanent set Two buckles merged Definite permanent set 2 buckles stayed in
0				
5.60	7			
10.07	6			
10.81				
0				
11.30	6			
0				
12.28	6			
0				
13.27*	6			
0				

*This represents the maximum capacity of the vacuum pump - failure was not achieved.

TABLE 13.- TENSILE TEST RESULTS.

1 Specimen No.	2 Area In. ²	3 Measured Thickness In.	4 E Psi x 10 ⁻⁶	5 Max. Load Ibs.	6 F _{tu} Psi	7 F _{ty} Psi	8 % Elongation (2" Gage Length)
1 AL	.00994	.0196	10.50	664	66,800	46,160	20.5
2 AL	.00994	.0196	11.45	661	66,500	45,440	18.5
1 AT	.01000	.0197	10.15	641	64,100	43,000	20.0
2 AT	.01000	.0197	9.97	638	63,800	41,360	18.0
1 BL	.00993	.0196	10.95	664	66,870	46,960	18.5
2 BL	.00994	.0196	9.83	665	66,900	45,600	17.0
1 BT	.00992	.0196	10.42	640	64,520	42,480	*
2 BT	.00992	.0196	10.04	640	64,520	41,600	17.5
1 CL	.01024	.0202	28.90	990	96,680	43,600	56.0
2 CL	.01024	.0202	24.00	1,000	97,660	44,160	60.5
1 CT	.01018	.0201	29.30	970	95,280	40,600	70.0
2 CT	.01020	.0201	29.80	975	95,590	42,400	68.5
1 DL	.01570	.0310	10.90	1,080	68,790	52,560	18.5
2 DL	.01572	.0310	10.92	1,100	69,970	53,360	18.0
1 DT	.01567	.0310	10.90	1,045	66,690	45,760	21.5
2 DT	.01567	.0310	10.60	1,045	66,690	44,400	*

TABLE 13.- Cont'd.

1 Specimen No.	2 Area In ²	3 Measured Thickness In.	4 E Psi x 10 ⁻⁶	5 Max. Load Lbs.	6 F _{tu} Psi	7 F _{ty} Psi	8 % Elongation (2" Gage Length)
1 EL	.01270	.0252	36.40	2,710	213,000	**	8.5
2 EL	.01260	.0252	27.50	2,700	214,000	**	*
3 EL	.01270	.0252	26.70	2,710	213,000	195,500	*
1 ET	.01260	.0252	34.40	2,800	222,000	**	14.5
2 ET	.01260	.0251	31.70	2,800	222,000	182,500	*
3 ET	.01260	.0251	29.70	2,810	223,000	180,000	10.0

- NOTE:
1. * - Elongation not given because specimen broke outside gage length.
 2. ** - Yield strength not obtained because of equipment failure.
 3. - At least two tensile specimens were taken in each grain direction from each sheet of material used.

SYMBOLS: L - parallel to grain

T - cross grain

- A - specimen taken from material used to make cones # 2, 3 & 4. 2024-T3 Clad Al.
 B - taken from material used to make cones # 5, 6, 7 & 8. 2024-T3 Clad Al.
 C - taken from cone # 10 material. 302 stainless steel.
 D - taken from material used to make cone # 9 & cylinder # 11. 2024-T3 Clad Al.
 E - taken from material used to make cone # 12. 301 full hard stainless steel.

TABLE 14.- STANDARDIZATION OF TEST RESULTS

Specimen No.	Measured bucking range P_{bm}		P_m	Standardized Buckle Range P_{bs}		P_m
2	1.72	2.33	—	1.71	2.31	—
3	1.67	2.19	—	1.66	2.17	—
4	.98	2.06	—	.97	2.05	—
5	1.11	—	—	1.13	—	—
6	.86	1.23	—	.88	1.25	—
7 U	2.45	2.75	2.94	2.57	2.89	3.01
7 L	1.42	2.45	—	1.41	2.44	—
8 U	2.35	2.94	3.58	2.31	2.88	3.64
8 L	1.91	2.16	—	2.01	2.27	—
9	4.22	—	—	4.22	—	—
10	3.10	—	—	2.55	—	—
11	3.98	4.52	—	3.98	4.52	—
12	6.14	—	—	4.25	—	—

NOTE: P_m - pressure at which 2 buckle patterns merged.

TABLE 15.- COMPARISON OF ULTIMATE PRESSURES
(Theoretical and Experimental Results)

Specimen No.	Experimental ¹ Results, P _u	Theoretical Results Lockheed
2	5.26	4.92
3	5.13	4.92
4*	10.46 +	4.92
5	3.14	3.26
6	3.09	3.26
7u**	—	7.30
7L	5.70	4.92
8u**	—	7.30
8L	5.64	4.92
9	8.97	9.32
10	5.29	7.02
11	11.89	8.20
12	13.27 +	13.50

¹Experimental Results were not Standardized.

*Had 4 heavy equally spaced stiffeners on outside

**Did not fail

TABLE 16.- COMPARISON OF INITIAL BUCKLING PRESSURES

(Theoretical and Experimental Results)

Speciman No.	Experimental Results P _b	Theoretical Results				
		Seide Approx.	Hart	Seide's Exact	NACA TR-874	Bijlaard
2	1.71 - 2.31	2.38	1.61	2.48	2.47	2.40
3	1.66 - 2.17	2.38	1.61	2.48	2.47	2.40
4	.97 - 2.05	2.38	1.61	2.48	2.47	2.40
5	1.13	1.45	1.03	1.46	1.46	1.31
6	.88 - 1.25	1.45	1.03	1.46	1.46	1.31
7u	2.57 - 2.89	3.66	2.49	3.76	3.76	3.57
	3.01*					
7L	1.41 - 2.44	2.38	1.61	2.48	2.47	2.40
8u	2.31 - 2.88	3.66	2.49	3.76	3.76	3.57
	3.64*					
8L	2.01 - 2.27	2.38	1.61	2.48	2.47	2.40
9	4.22	4.71	3.18	4.80	4.76	4.29
10	2.55	3.78	2.57	3.69	3.69	3.40
11	3.98 - 4.52	5.89	5.09	6.00	5.99	6.15
12	6.14	6.60	4.44	6.52	6.50	6.94

* - P_m - Pressure at which upper and lower buckle patterns merged.

TABLE 17.- PERCENTAGE VARIATION BETWEEN TEST AND THEORETICAL RESULTS

Specimen No.	Ultimate Pressure	Initial Buckling Pressure				
	Lockheed	Seide's Approx.	Seide's Exact	Hart	NACA TR-874	Bijlaard
2	-6.4	+38.8	+45.0	-5.85	+44.4	+40.4
3	-4.1	+43.3	+49.4	-3.01	+48.8	+44.6
4	NA	NA	NA	NA	NA	NA
5	+3.8	+28.3	+29.2	-8.84	+29.2	+15.9
6	+5.2	+64.8	+66.0	+17.1	+66.0	+48.9
7u	NA	+42.2	+46.3	-3.11	+46.3	+38.9
7L	-13.7	+68.8	+75.8	+12.4	+75.2	+70.2
8u	NA	+58.5	+62.8	+ 7.8	+46.3	+54.5
8L	-12.5	+18.4	+23.4	-19.8	+22.9	+19.4
9	-3.91	+16.5	+13.8	-24.7	+12.8	+ 1.6
10	+32.7	+48.3	+44.7	+ 0.8	+44.7	+33.3
11	-31.0	+48.0	+50.7	+27.9	+50.5	+54.6
12	NA	+ 7.5	+ 6.2	-27.7	+ 5.9	+13.0

NA - Not applicable because specimen did not fail or had stiffeners on outside.

10.0 FIGURES

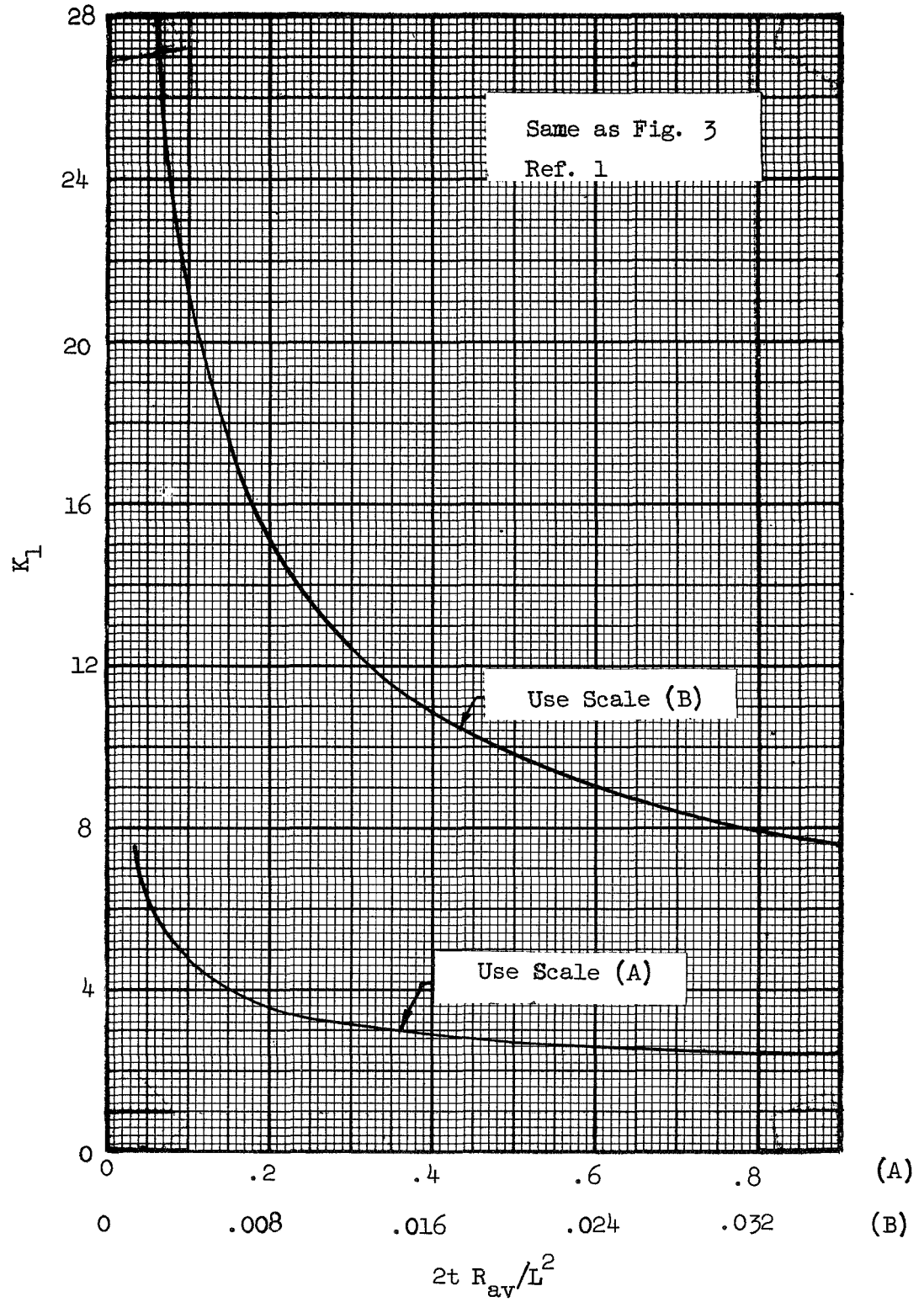


Figure 1.- Plot of Thickness-Radius-Length Parameter vs K_L

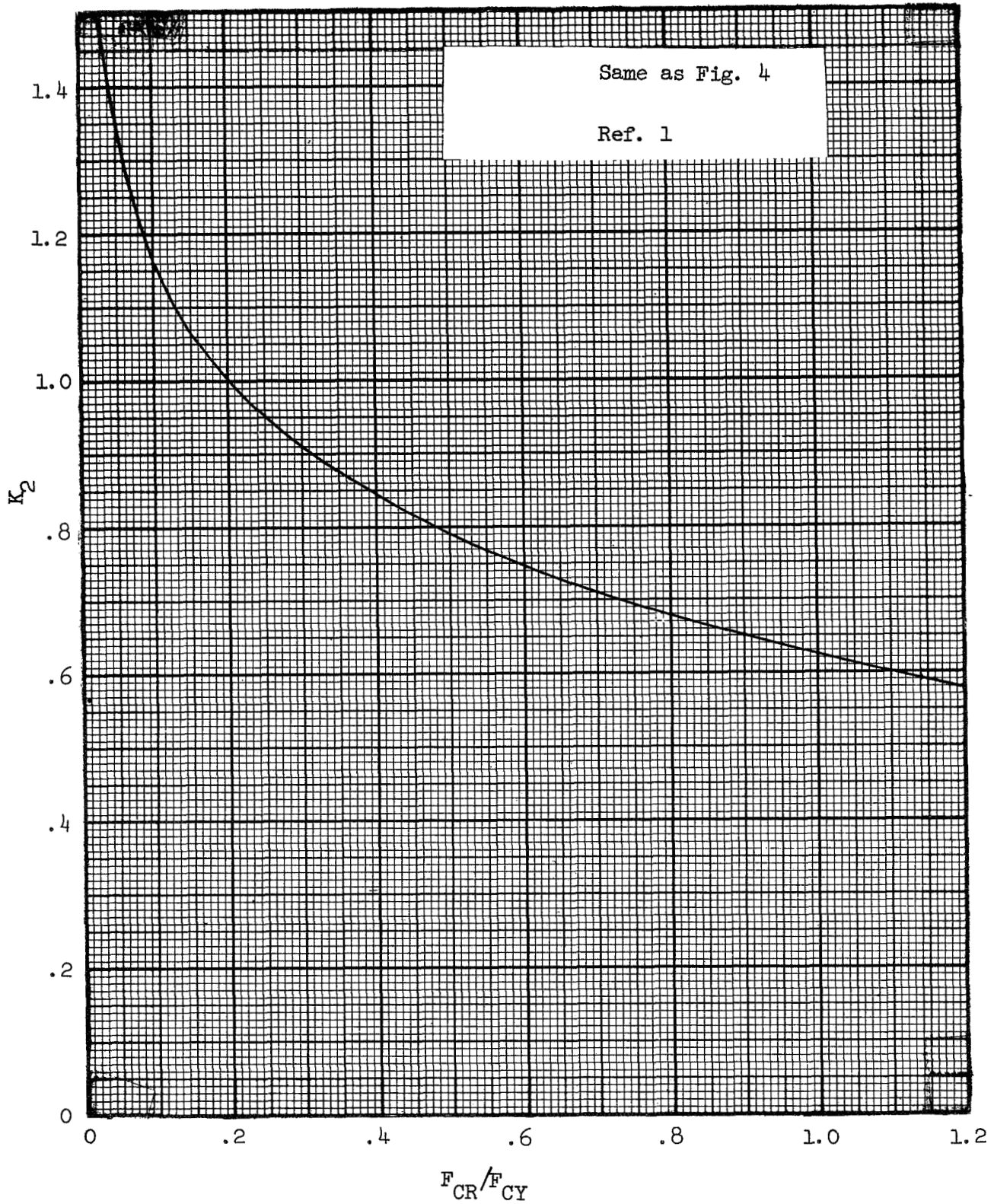


Figure 2.— Plot of Non-Dimensional Shape Factor Vs Critical-
Compressive Stress Ratio.

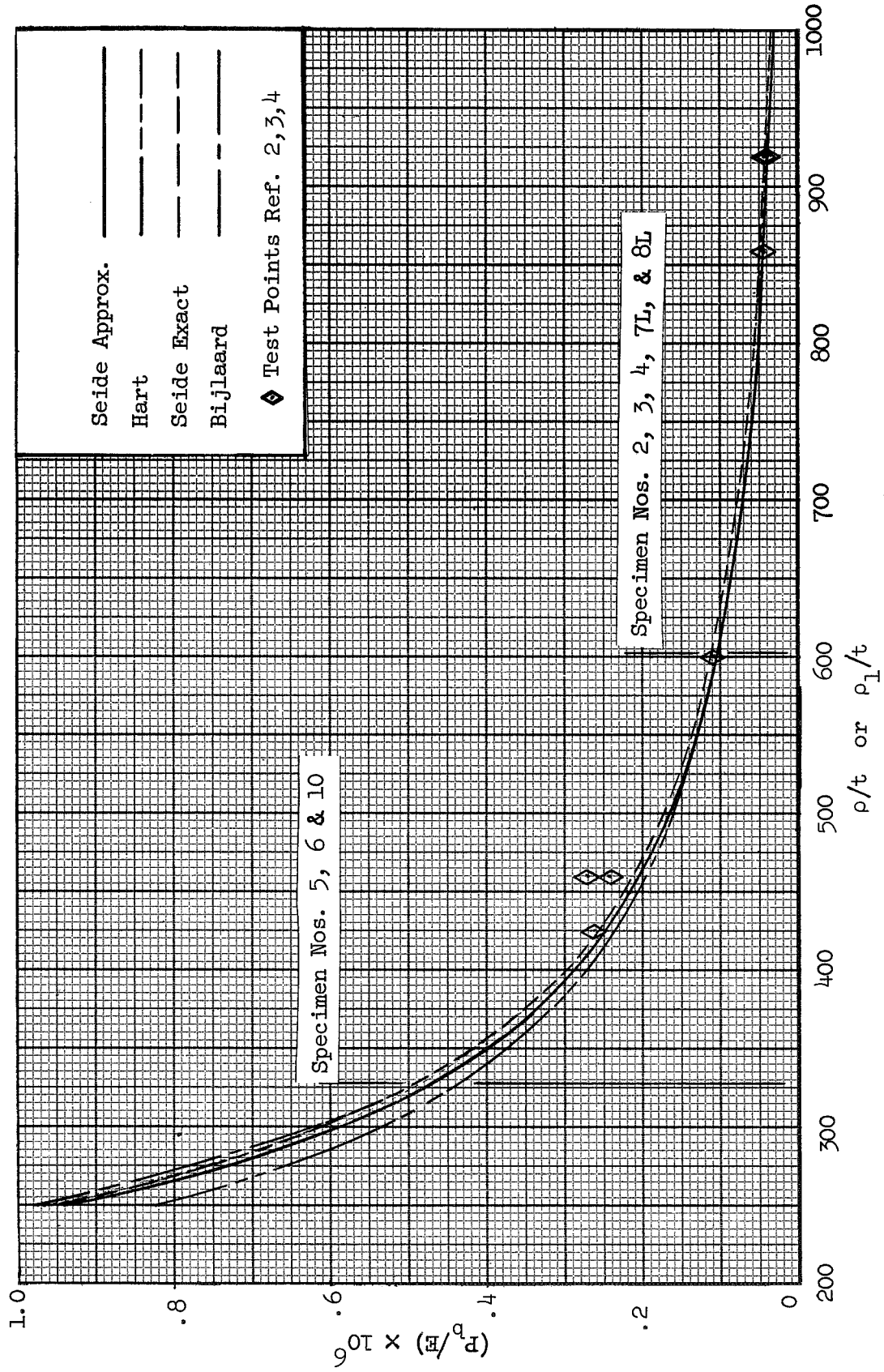


Figure 3.— Comparison of Available Analytical Data on 30° Half Angle Conical Frustums.

$$L'/\rho_1 \quad \text{or} \quad I_{eq}/\rho = 1.0; \quad \nu = .3$$

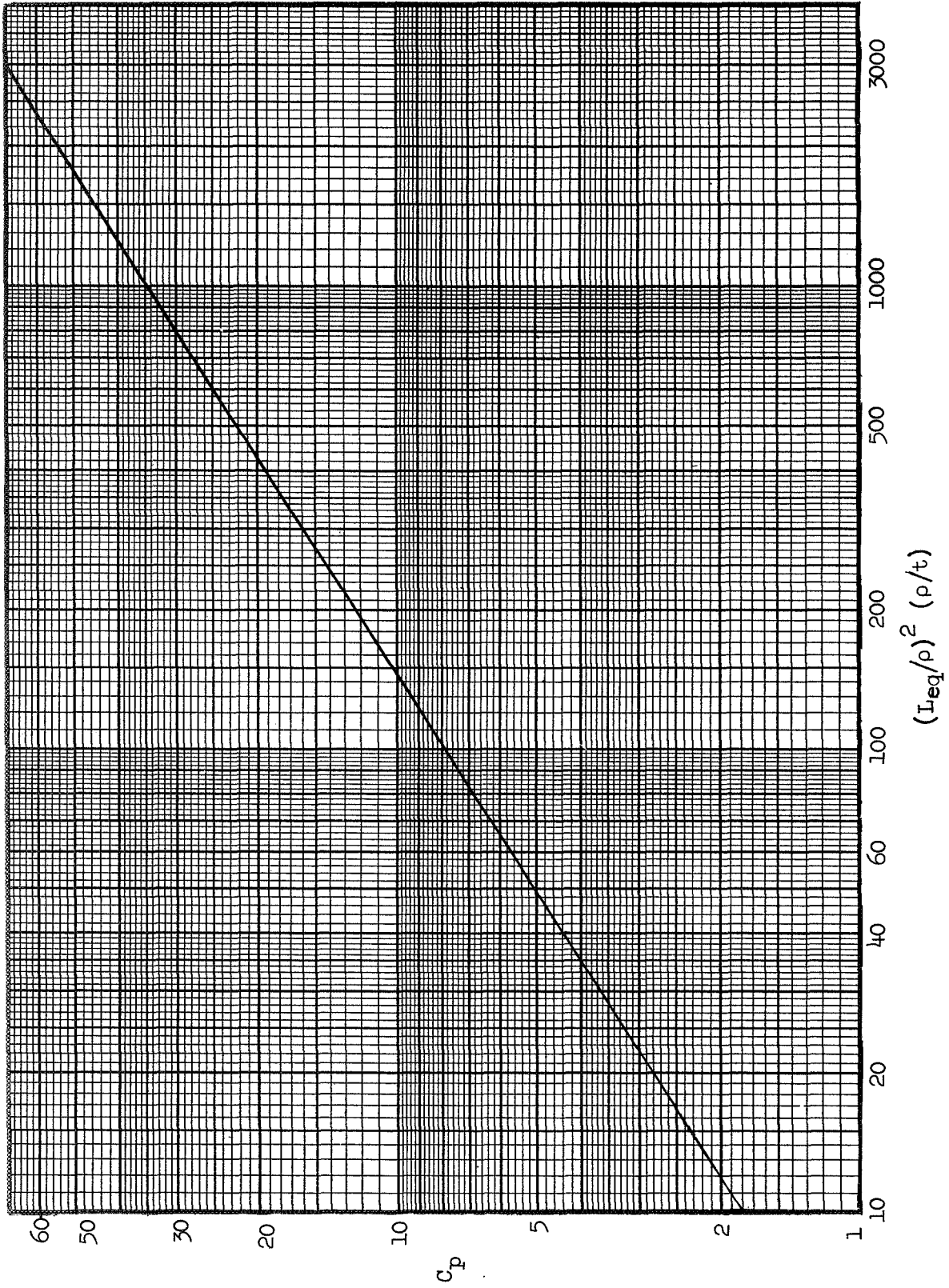


Figure 4.— External Buckling Pressure Coefficient vs Length-Radius-Thickness Parameter

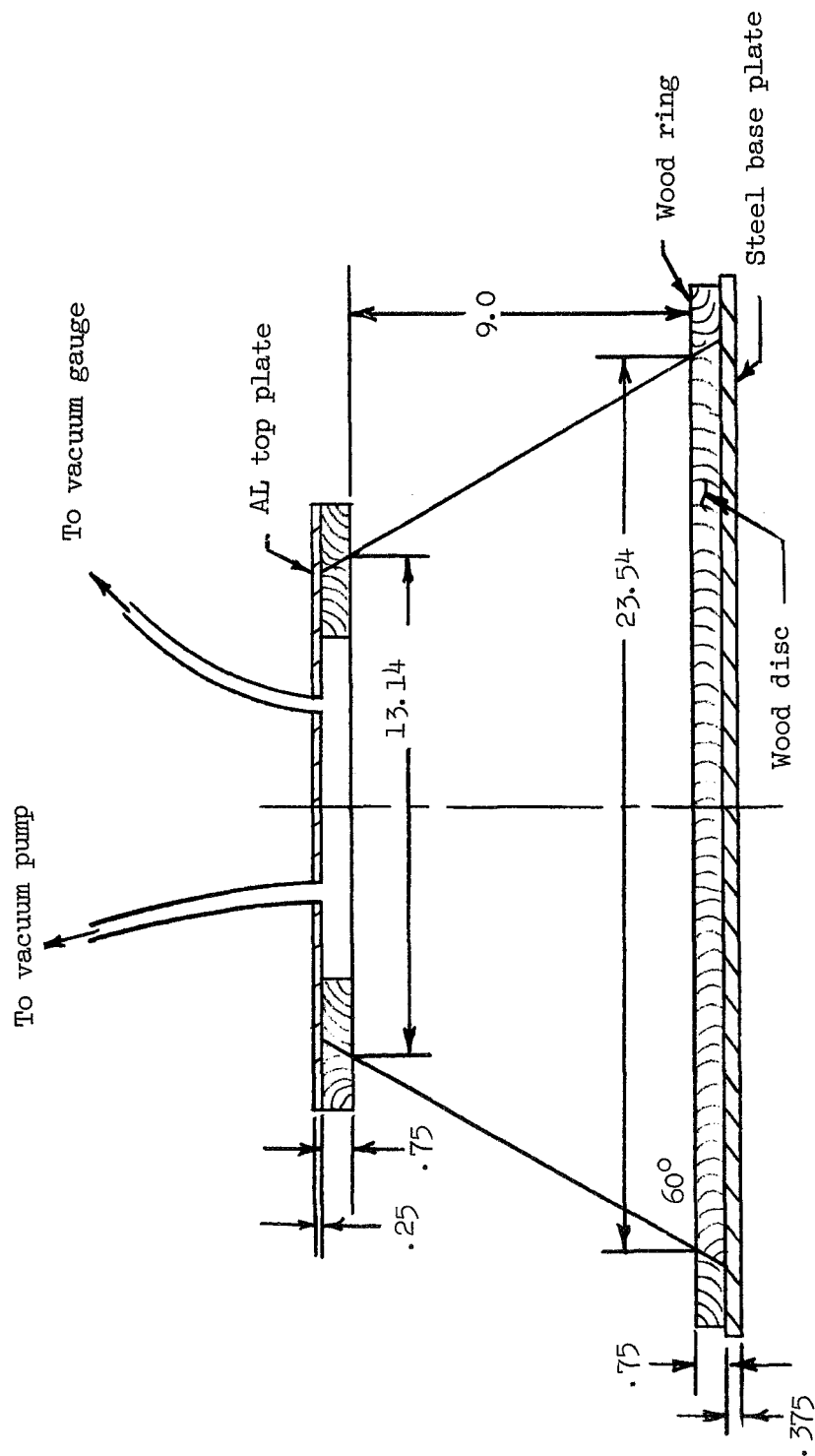


Figure 5. - Typical Test Setup.

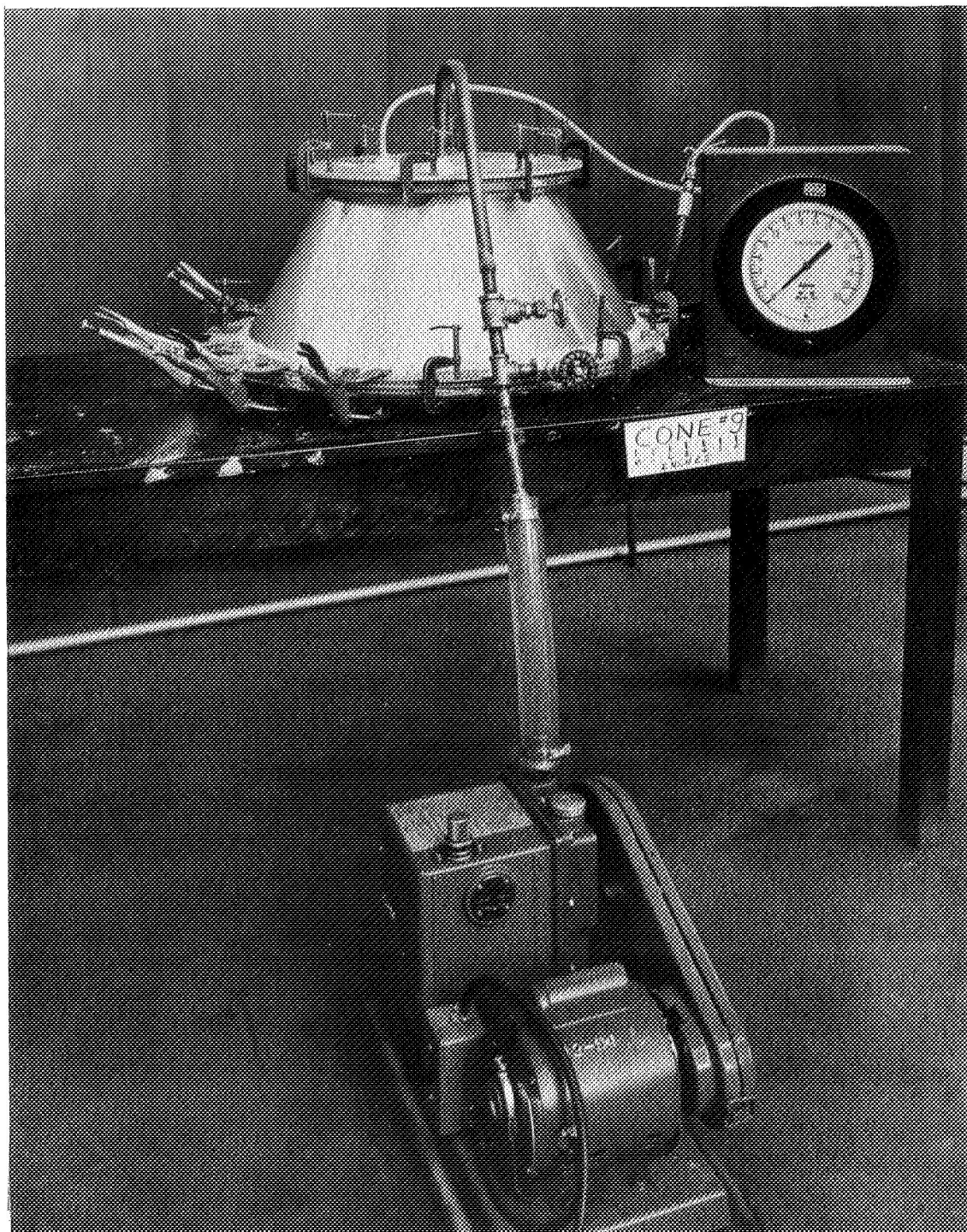


Figure 6. - Test Arrangement

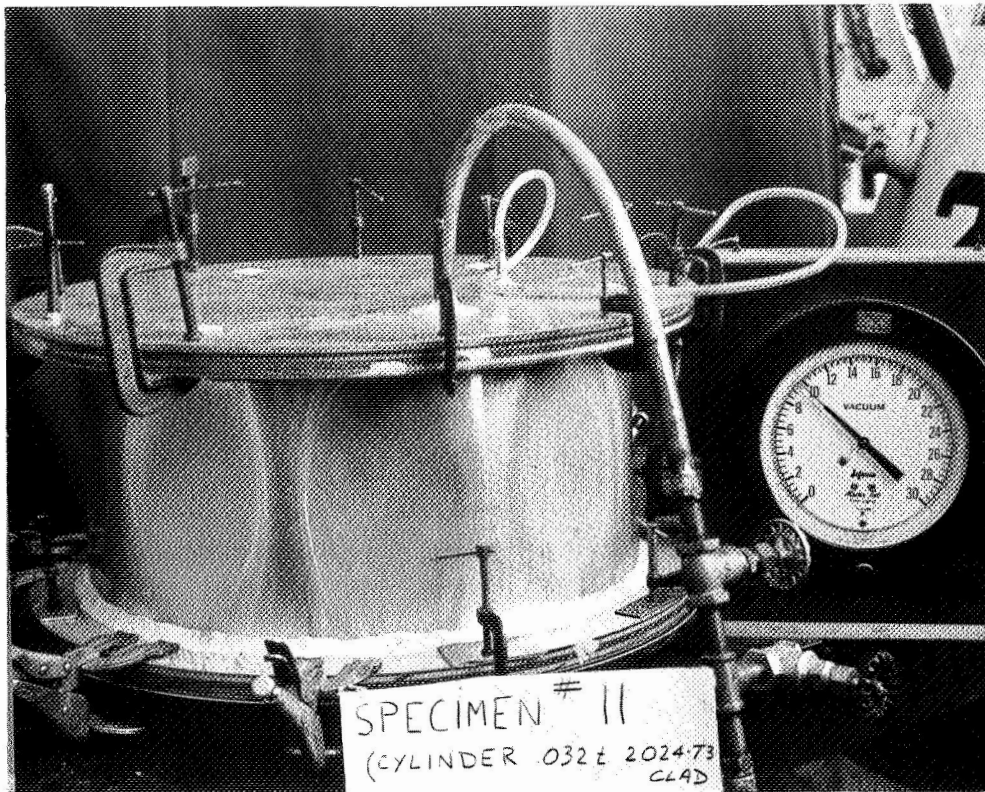


Figure 7.- Elastic Buckles in Cylindrical Specimen

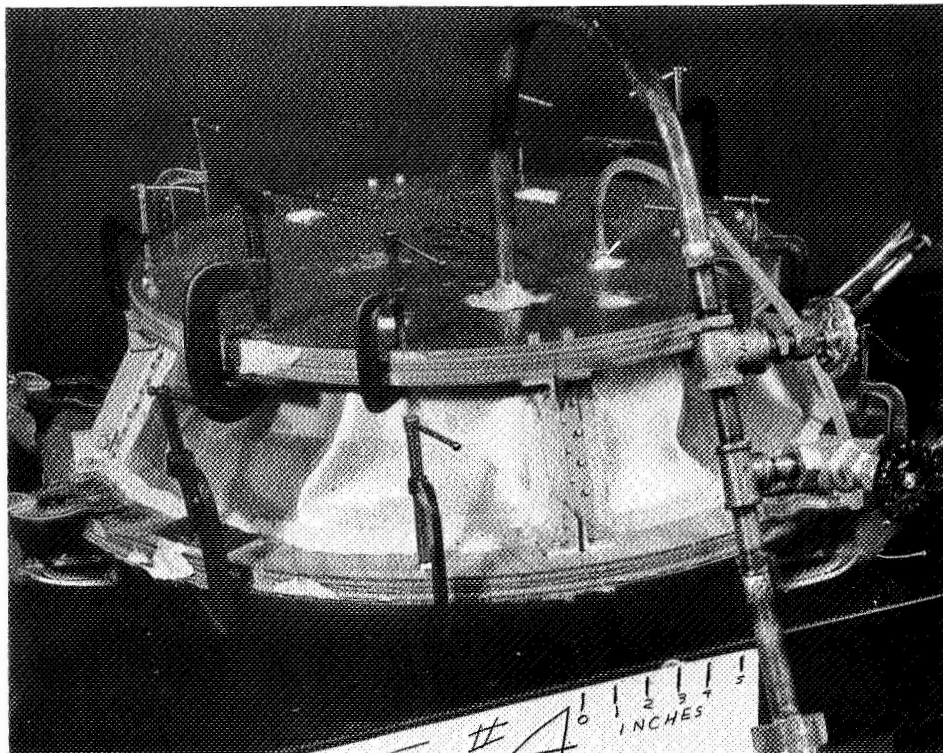


Figure 8.- Buckle Pattern on Stiffened Shell
(Cone No. 4 at 7.8 psi)

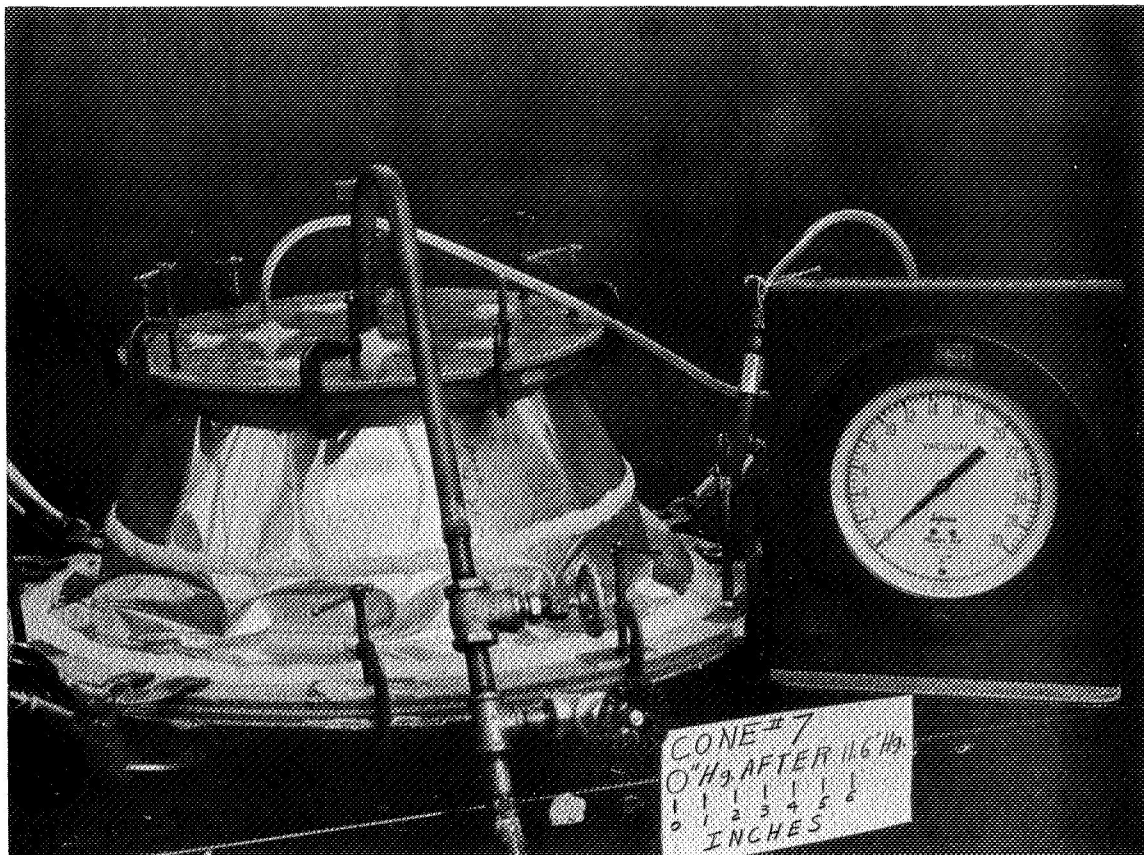


Figure 9.- Failure of Lower Bay Together with Permanent Set in Upper Bay

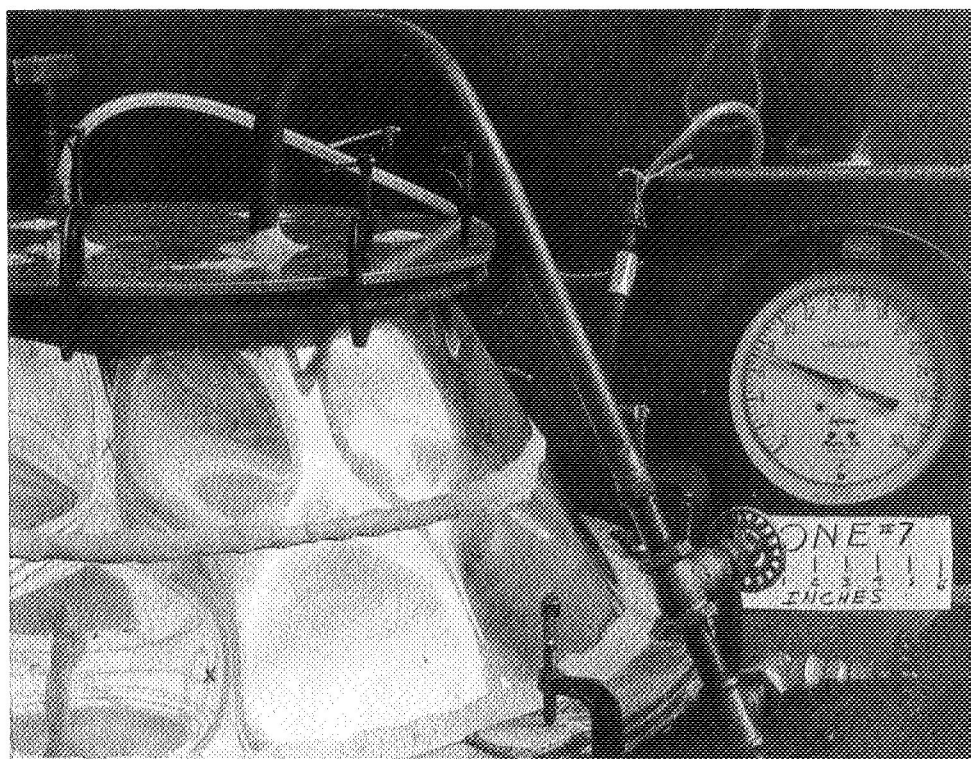


Figure 10.- Interaction of Buckle Patterns on Multi-Bay Specimen

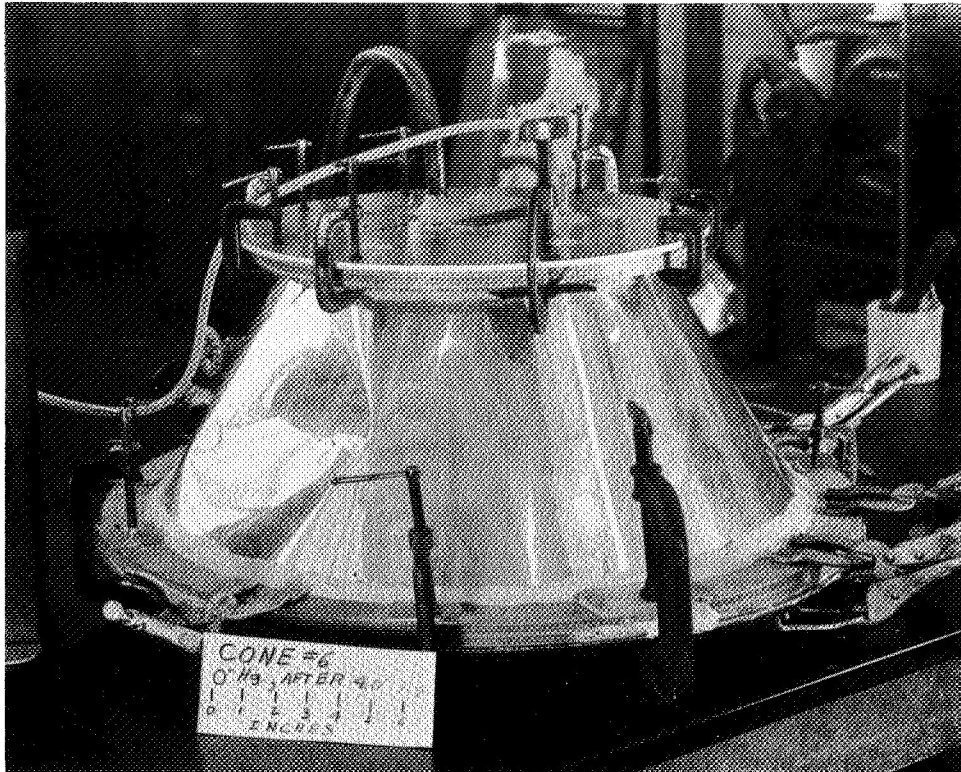


Figure 11.- Permanent Buckle After Release of Pressure

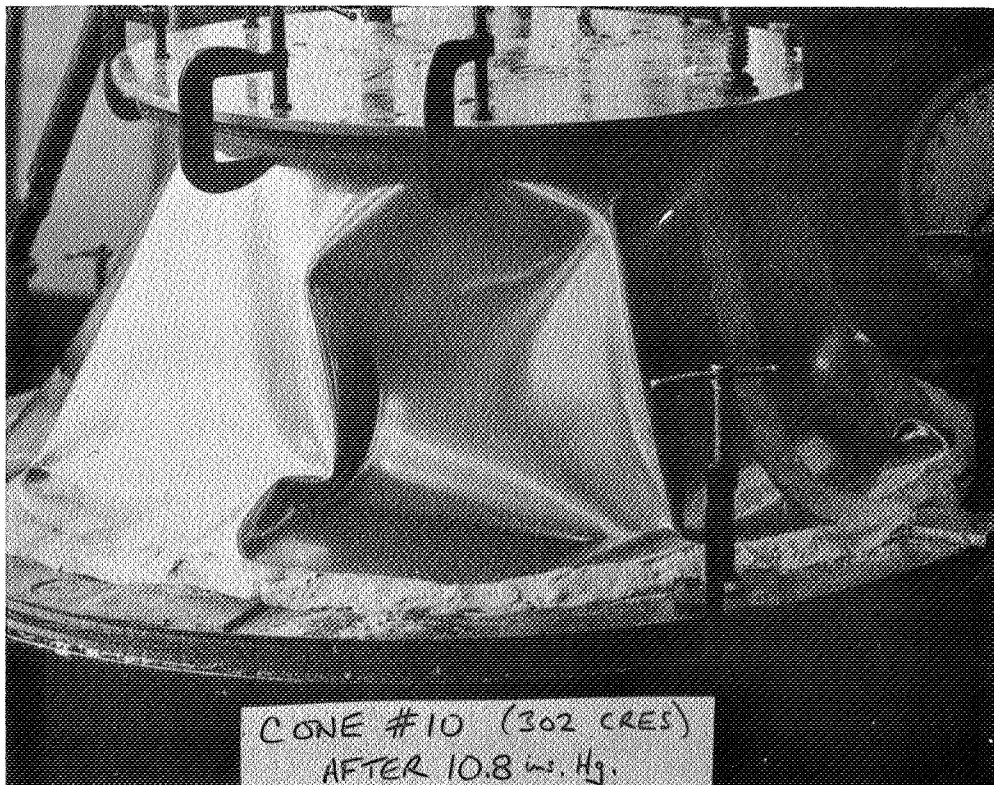


Figure 12.- Failure of Stainless Steel Specimen

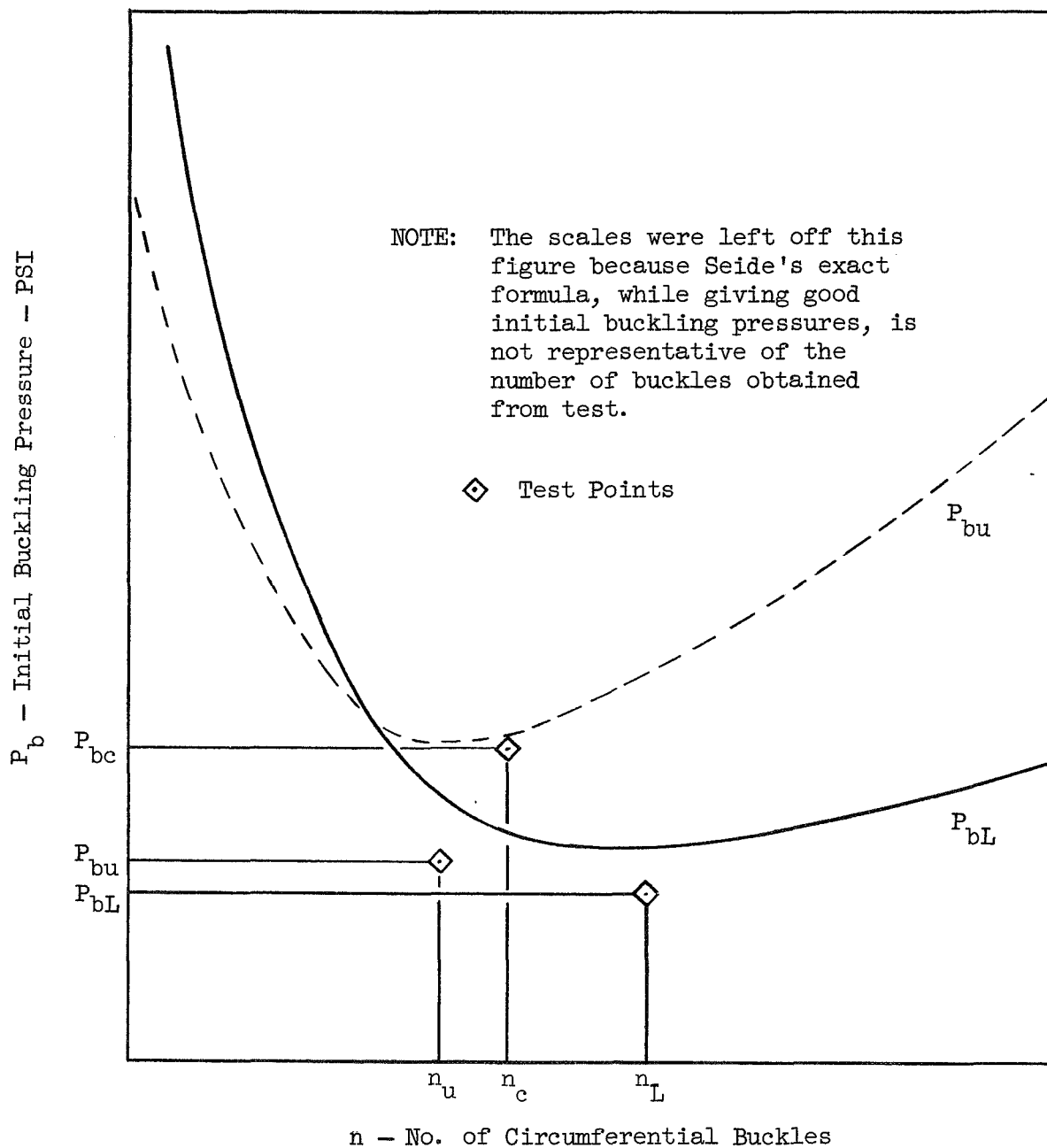


Figure 13.- Initial Buckling Pressures vs No. of Circumferential Buckles Based on Seide's Exact Formula for Multi-Bay Conical Shell (Specimen No. 8) Showing Test Results

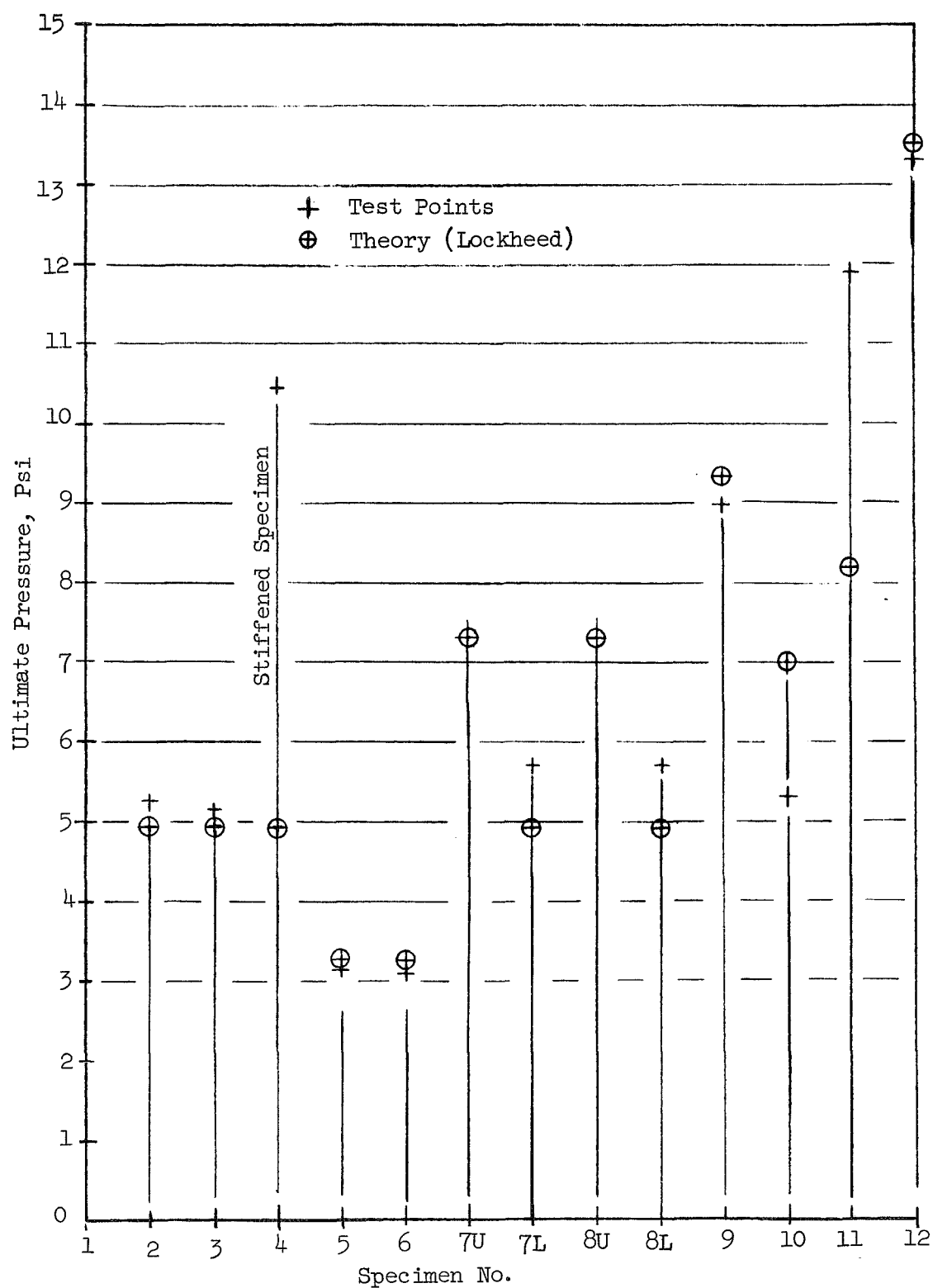


Figure 14.- Comparison of Ultimate Pressure between
Experimental and Theoretical Results.

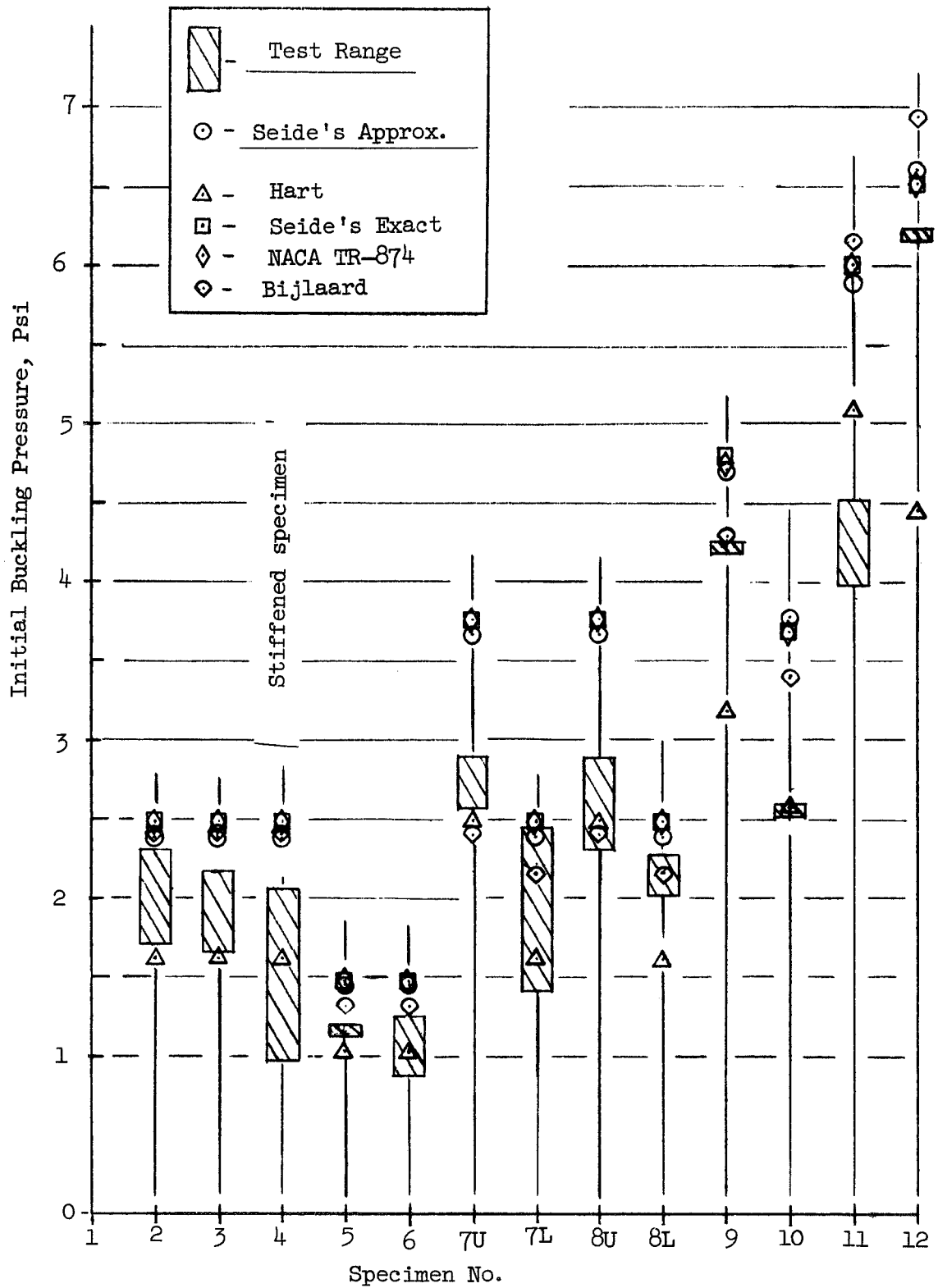


Figure 15.- Comparison of initial Buckling Pressure between Experimental and Theoretical Results. (Lower edge of test range taken as initial buckling pressure)

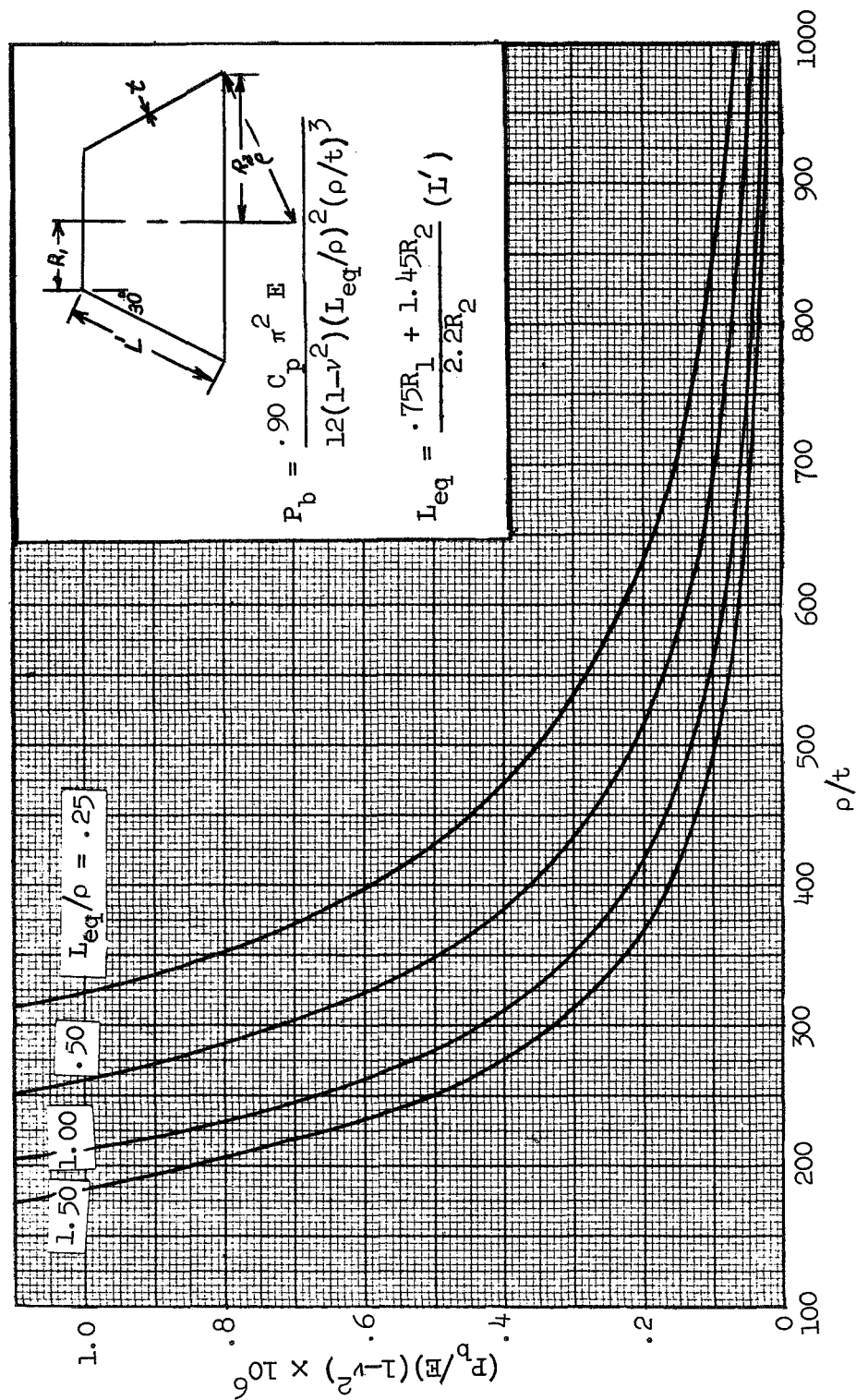


Figure 16.— Design Curve for Determining Initial Buckling Pressure on 30° Half Angle Conical Frustums Using "Hart's" Method.